ANNALI DI GEOFISICA, VOL. XXXVIII, N. 2, May 1995

Analysis of strong-motion data of the 1990 Eastern Sicily earthquake

Massimo Di Bona ([1]), **Massimo Cocco** ([1]), **Antonio Rovelli** ([1]), **Raniero Berardi** ([2]) **and Enzo Boschi** ([1])
([1]) *Istituto Nazionale di Geofisica, Roma, Italy*
([2]) *Ente Nazionale per l'Energia Elettrica (ENEL), Roma, Italy*

Abstract
The strong motion accelerograms recorded during the 1990 Eastern Sicily earthquake have been analyzed to investigate source and attenuation parameters. Peak ground motions (peak acceleration, velocity and displacement) overestimate the values predicted by the empirical scaling law proposed for other Italian earthquakes, suggesting that local site response and propagation path effects play an important role in interpreting the observed time histories. The local magnitude, computed from the strong motion accelerograms by synthesizing the Wood-Anderson response, is $M_L = 5.9$, that is sensibly larger than the local magnitude estimated at regional distances from broad-band seismograms ($M_L = 5.4$). The standard omega-square source spectral model seems to be inadequate to describe the observed spectra over the entire frequency band from 0.2 to 20 Hz. The seismic moment estimated from the strong motion accelerogram recorded at the closest rock site (Sortino) is $M_0 = 0.8 \times 10^{24}$ dyne·cm, that is roughly 4.5 times lower than the value estimated at regional distances ($M_0 = 3.7 \times 10^{24}$ dyne·cm) from broad-band seismograms. The corner frequency estimated from the acceleration spectra is $f_c = 1.3$ Hz, that is close to the inverse of the duration of displacement pulses at the two closest recording sites. This value of corner frequency and the two values of seismic moment yield a Brune stress drop larger than 500 bars. However, a corner frequency value of $f_c = 0.6$ Hz and the seismic moment resulting from regional data allows the acceleration spectra to be reproduced on the entire available frequency band yielding to a Brune stress drop of 210 bars. The ambiguity on the corner frequency value associated to this earthquake is due to the limited frequency bandwidth available on the strong motion recordings. Assuming the seismic moment estimated at regional distances from broad-band data, the moment magnitude for this earthquake is 5.7. The higher local magnitude (5.9) compared with the moment magnitude (5.7) is due to the weak regional attenuation. Beside this, site amplifications due to surface geology have produced the highest peak ground motions among those observed at the strong motion sites.

Key words *strong motion – site amplification – stress drop – spectral analysis – anelastic attenuation*

1. Introduction

On December 13, 1990 at 00:24 GMT, Eastern Sicily was struck by an earthquake which caused huge damage and several fatalities. Despite the low value of the coda magnitude ($M_D = 4.7$), estimated on the short-period seismometers of the ING National Network, the earthquake was felt in a wide area. The local magnitude is $M_L = 5.4$, as estimated from the synthetic Wood-Anderson seismograms obtained by the very broad-band data recorded at regional distances from the seismic stations of the MEDNET network (Salvatore Mazza and Andrea Morelli written communication, 1991). This magnitude value appears still to be inconsistent with the actual severity of the shock. The earthquake was localized 8 km off-shore the Augusta promontory (Amato *et al.*, 1994). The aftershock sequence was unusual: only a few aftershocks occurred within three days of the main shock; the aftershock sequence began on December 16 when an $M_L = 4.6$ event oc-

curred (Cocco *et al.*, 1991). The focal mechanism computed both from first motion polarities (Amato *et al.*, 1994) and from the inversion of broad-band waveforms (Giardini *et al.*, 1994) shows a strike slip solution (see fig. 1).

The Eastern Sicily earthquake triggered eight SMA-1 accelerometers of the ENEL network within 120 km from the epicentre. The SMA-1 recordings were digitized using a high resolution optical scanner (400 sps) by the ENEA-ENEL Joint Commission. These recordings represent an unprecedented data set for evaluating some physical quantities of the ground motion produced by an intermediate size earthquake in Eastern Sicily. Moreover, the strong-motion data represent an important tool to clear up the disagreement between the magnitude estimates and the severity of the earthquake.

The Italian strong motion data set was previously analyzed in order to obtain a parameterization of the ground motion spectrum in the frequency range of engineering interest (0.5 – 20 Hz) and to investigate the scaling laws between peak ground motions versus focal distance and earthquake size (Rovelli *et al.*, 1988, 1991). This data set is comprehensive of normal faulting events which occurred along the Apennines and of thrust faulting events which occurred in the north-eastern Alps (Friuli). The 1990 Eastern Sicily earthquake is one of the first strike slip events in Italy for

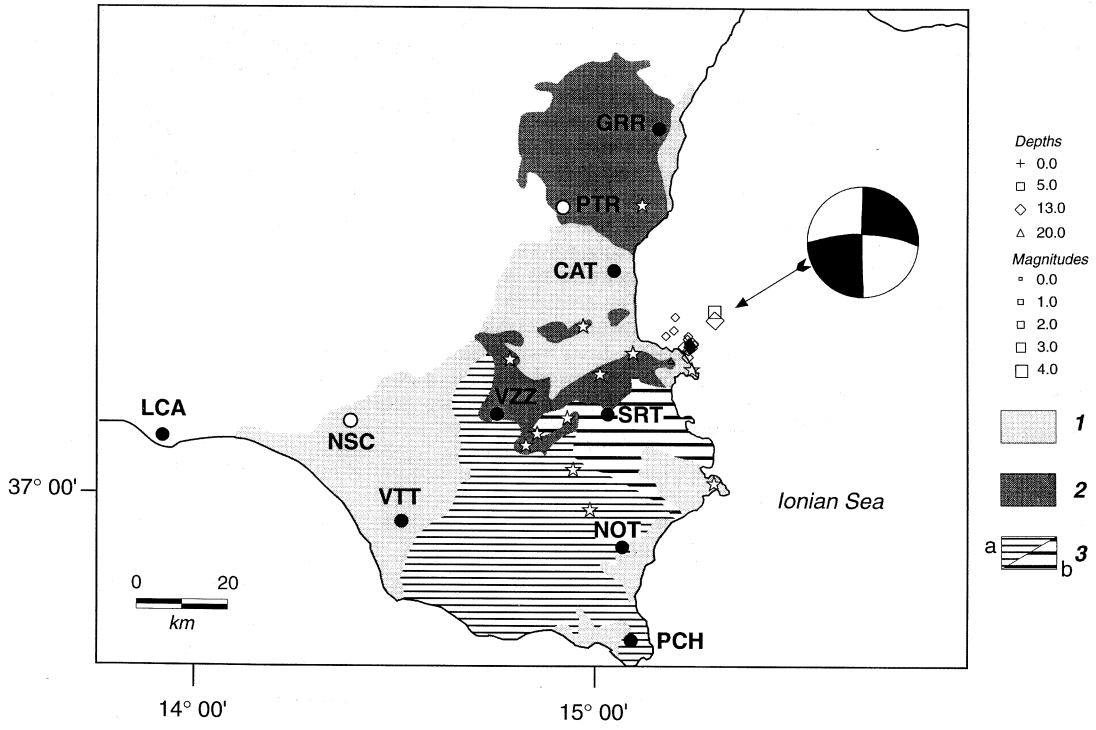

Fig. 1. Distribution of seismometric (stars) and accelerometric (circles) stations operating in the area. Solid circles indicate the triggered accelerographs, while open circles show the two accelerographs that were not activated by the main shock. The main geologic features of the area have been drawn: 1) Quaternary marine and continental sediments; 2) Etna and Iblean platform basic volcanic rocks; 3) Carbonate units of the Iblean foreland. The epicentral locations of the main shock and of the aftershocks, and the mainshock focal mechanism are also shown.

which good quality strong motion data are available.

In this paper we analyze the accelerograms written by the 1990 Eastern Sicily earthquake in order to estimate both seismological and engineering parameters, such as peak ground motions, seismic moment, stress drop as well as the attenuation parameters. We discuss the different contributions to the observed ground motions coming from the source, the anelastic attenuation and the local site response. Finally, we compare these estimates with the scaling laws and the spectral models obtained by analyzing the strong motion data from other earthquakes which have occurred in Italy.

2. The data set

The 1990 Eastern Sicily earthquake was recorded by eight strong motion accelerometers deployed by the Italian Electric Company (ENEL). Each station is equipped with a SMA-1 accelerograph that records ground acceleration on a 70 mm photographic film. The film traces were automatically digitized using a high resolution optical scanner with a sampling rate of 400 sps. This data set was processed by the ENEA-ENEL Joint Commission. Figure 1 shows the distribution of both accelerometric and seismometric stations, which were operating in the area immediately after the earthquake, and the main geologic features of this area. The ING deployed a temporary network consisting of both short-period and broad-band seismometers immediately after the mainshock, allowing the recording of the aftershock sequence. Figure 1 also shows the mainshock and aftershock epicentral locations (Amato *et al.*, 1994) and the mainshock focal mechanism (Giardini *et al.*, 1994; Amato *et al.*, 1994). Unfortunately, the aftershocks did not trigger the strong motion instruments due to their small magnitudes. The strong motion data set includes only the mainshock recordings. The three components of the ground displacement and velocity were computed from the recorded ground acceleration using the numerical procedure proposed by Alessandrini *et al.* (1990). The acceleration, velocity and displacement peak values (the maximum among the three components) and the hypocentral distances for the mainshock are listed in table I.

Table I. Peak ground motions at the accelerometric sites.

Station	Code	R (km)	a_p (gal)	v_p cm/s	d_p cm	Site
Sortino	SRT	32	102	6.9	1.3	Miocene pyroclastic rocks
Catania	CAT	29	247	9.3	1.7	Holocene alluvial sands and clays, thickness greater than 50 m
Vittoria	VTT	80	28	1.9	0.3	Middle Pleistocene sands and clays thickness greater than 30 m overlaying calcarenites
Giarre	GRR	49	39	6.1	0.6	Etna basaltic lava flows
Vizzini	VZZ	51	73	4.2	0.5	Upper Miocene basaltic lava flows
Pachino	PCH	73	59	2.5	0.2	Cretaceous thephritic lava flows
Noto	NOT	54	88	5.1	0.6	Calcarenites
Licata	LCA	122	41	2.8	0.2	Alluvial sands and clays thickness of about $\approx$ 10 m, overlaying Pleistocene marls and clays

Figure 2 shows the *NS* components of the acceleration time histories for seven stations (the recording from Licata site is not included in the figure). The time scale is measured relative to the earthquake origin time T_0. The triggering time t_0 for each accelerometer was given by the instrument's internal clock, with an accuracy of ± 1 s, and listed in table II.

Because the triggering time of the Vittoria accelerometer (VTT) was not available, we computed a theoretical triggering time for all the accelerometric stations; the theoretical value for Vittoria has been used in fig. 2. The theoretical triggering times are computed using the following equation

$$t_0^c - T_0 = (t_S - T_0) - (t_S - t_0) \qquad (2.1)$$

where $t_S - T_0$ is the *S*-wave travel time at each

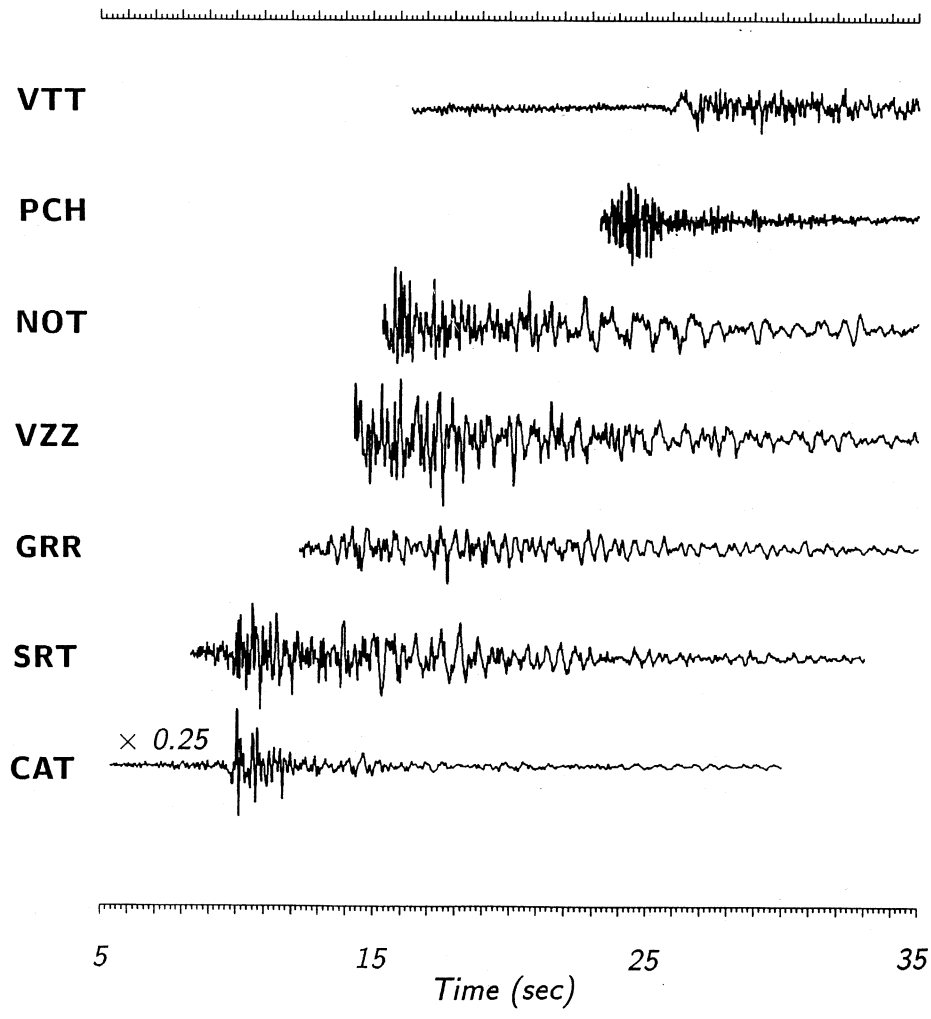

Fig. 2. NS component of ground acceleration recorded at seven sites of the ENEL network. The waveforms have been aligned with respect to the earthquake origin time. The time history recorded at the Licata site is not included in this figure.

Table II. Triggering times.

Code	Activation time (GMT)	$t_0 - T_0$ (s)	$t_0^c - T_0$ (s)
SRT	00:24:38	9.0	8.2
CAT	00:24:35	6.0	5.3†
VTT			15.1
GRR	00:24:42	13.0	14.0
VZZ	00:24:44	15.0	16.0★
PCH	00:24:53	24.0	22.0★
NOT	00:24:45	16.0	16.9★
LCA	00:25:08	39.0	37.5★

★ Accelerograph triggered by *S*-waves; † computed with $\beta = 3.0$ km/s.

station, and $t_S - t_0$ is the arrival time of the *S*-wave after the triggering time (t_0). The travel times were computed using the hypocentral location and the best half-space velocity model proposed by Amato *et al.* (1994). The *S*-wave arrivals $t_S - t_0$ were read from the recordings of the horizontal ground acceleration. For the accelerometers triggered by the *S*-waves, we assumed that the direct *S*-wave triggered the instrument. In this situation we set $t_S - t_0 \approx -0.5$ s, that corresponds to the mechanical delay time between the triggering time and the beginning of the recording. Instrumental triggering times are computed by the activation time available from the accelerographs and the origin time resulting from the earthquake location procedure (00:24:29, see Amato *et al.*, 1994). Both the instrumental and the theoretical triggering times are listed in table II. Even if these values agree within the time accuracy of the instruments (± 1 s) for most of the stations, there is some ambiguity for the Catania recording. In fact, the *S*-wave arrival time after the instrument triggering on the Catania recording is $t_S - t_0 = 4.4$ s. By assuming a *P*-wave velocity equal to 5.9 km/s and an *S*-wave velocity equal to 3.3 km/s (as proposed by Amato *et al.*, 1994) and a hypocentral distance of 29 km, we find that the *S*-wave travel time is $t_S - T_0 = 8.8$ s that corresponds (eq. (2.1)) to a triggering time of 4.4 s. This value of the triggering time is paradoxically less than the *P*-wave travel time, that is 4.9 s. Two sources of error can be invoked in order to explain this self-contradiction. The first one is an error in the hypocentre location: increasing the hypocentral distance by 5 km leads to a theoretical triggering time equal to 6.2 s, greater than the value 5.9 s obtained for the *P*-wave travel time and closer to the instrumental triggering time value (6.0 s). However, Amato *et al.* (1994) located the Syracuse main shock using a master event algorithm and found location errors of the order of 2 km. The second explanation is to suppose that the *S*-wave velocity in the Catania plane, located near the Etna volcano, is lower than the mean value suggested by Amato *et al.* (1994). A trial value of 3.0 km/s for the *S*-wave velocity leads to a computed triggering time equal to 5.3 s (this value has been included in table II). In both cases the time difference between the instrument activation time and the *P*-wave arrival is within 0.3 s, that is less than the mechanical delay time of the accelerograph.

The interpretation of ground motions recorded at the Catania and Sortino sites, that are at similar hypocentral distances but opposite local site conditions, plays an important role in understanding the attenuation and the source mechanisms for this earthquake. The analysis of surface geology (shown in fig. 1) points out the presence of relevant crustal heterogeneities in the area. Consequently, we expect that the near-receiver amplifications strongly influence the ground motions recorded at the accelerometric stations triggered by the earthquake. Moreover, we should expect that the propagation of seismic waves is affected by lateral variations of the attenuation properties of the crust. The two sites of Sortino and Catania recorded very different peak accelerations in spite of their comparable hypocentral distances (see table I). The two accelerographs are located in different geological conditions: the Sortino accelerometer is located on a rock site (volcanic rocks), while the Catania instrument is located on an alluvial plane near the Etna volcanic complex (see fig. 1). The surface geology of the Catania site consists of Holocene sediments characterized by a ≈ 10 m thick sand and clay layer overlying $30 \div 40$ m thick gravelly and sandy sediments; a deeper layer is

composed of Pleistocene marls and clays. Ground motion amplifications are expected at the Catania site under these geological conditions. Moreover, local site response certainly affected the ground acceleration recorded at Licata, 120 km away from the hypocentre. The Licata accelerometer recorded a peak acceleration of 40 gals (table I). This peak value is greater than the expected one for a moderate size earthquake at this distance. Moreover, two nearer accelerometers were not triggered by the earthquake (NSC and PTR in fig. 1, located at 80 and 45 km away from the epicentre, respectively), because the peak acceleration at these stations did not reach the triggering threshold value of 10 gals.

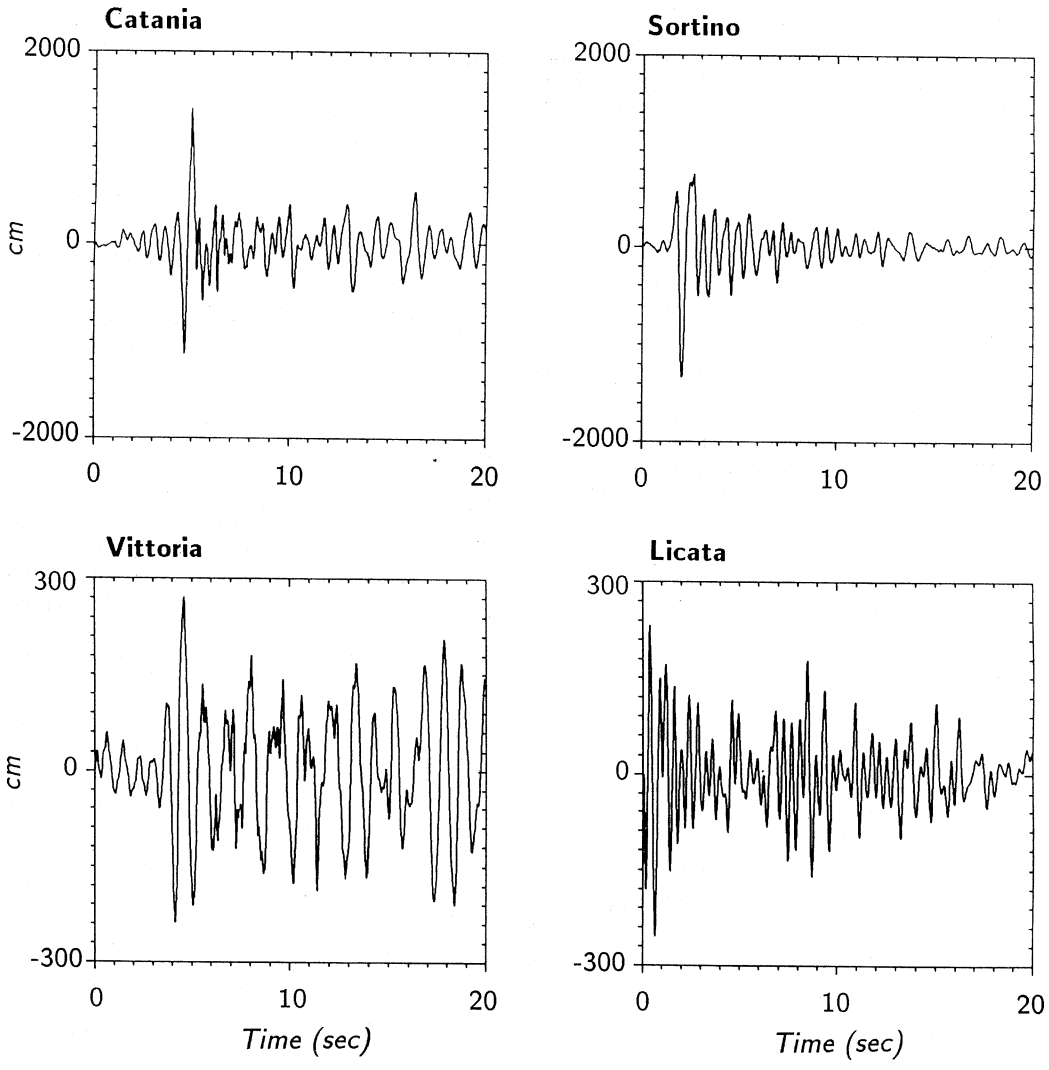

Fig. 3. Synthetic Wood-Anderson seismograms computed at four recording sites from the time histories of ground acceleration.

3. Local magnitude estimate from the strong-motion data

Kanamori and Jennings (1978) demonstrated that synthetic Wood-Anderson seismograms can be obtained from the strong-motion data allowing the estimate of local magnitude. This procedure has been tested for several earthquakes which occurred in California (see Hutton and Boore, 1987). Bonamassa and Rovelli (1986) applied this method to the strong-motion data recorded during recent Italian earthquakes. This procedure has been applied to the strong motion accelerograms recorded during the Eastern Sicily earthquake. Figure 3 shows some Wood-Anderson seismograms synthetized from the acceleration signals recorded at Catania, Sortino, Vittoria and Licata. The local magnitude estimates are listed in table III for all the stations. The mean value is $M_L = 6.3 \pm 0.3$, where the dispersion of the estimates is represented by one standard deviation.

This local magnitude value is much larger than the estimate obtained from the very broad-band data recorded at regional distances by the MEDNET network, that is $M_L = 5.4$. This difference is partly due to the site amplification which influenced the ground motion in some stations located on alluvial sediments (Catania and Licata), or to topographic effects that might have affected the recordings at some sites (Vizzini). The Sortino accelerograms, recorded on a rock site at 30 km from the source, produced the lowest local magnitude value (5.9 as average of the estimates from the two horizontal components). If we assume the absence of near-receiver amplifications at the Sortino site, the value $M_L = 5.9$ can be considered representative of the actual high frequency energy released by the earthquake. The difference between this value and the one estimated at regional distance (5.4) can be explained by low anelastic attenuation properties of the basaltic bedrock of the Iblean platform that controls the south-west propagation of seismic waves.

Table III. Source and attenuation spectral parameters.

Code	Component	M_L	κ $\times 10^{-2}$ s	f_c Hz	M_0 $\times 10^{24}$ dyne·cm
SRT	NS	5.8	4.0	1.5	0.7
	EW	6.1	3.2	1.1	0.9
CAT	NS	6.4	4.2	1.8	1.8
	EW	6.5	4.1	1.3	1.8
VTT	NS	6.5	3.6	0.9	1.3
	EW	6.3	2.9	0.9	1.7
GRR	NS	6.1	8.2	1.7	1.3
	EW	6.0	8.6	1.5	1.3
VZZ	NS	6.4	4.2	1.2	1.6
	EW	6.4	3.9	1.2	1.4
PCH	NS	5.8	4.7	1.9	0.9
	EW	6.2	3.9	2.0	0.9
NOT	NS	6.4	4.7	1.1	1.2
	EW	6.5	4.2	0.8	1.3
LCA	NS	6.8	13.		1.8
	EW	6.5	17.		1.5

4. Waveform analysis

In this section, we analyze the time histories recorded at the Sortino and Catania sites, because they are the two closest accelerographs and because they were both triggered by *P*-waves. As previously discussed, the interpretation of these two accelerograms is important in order to clear up the source, propagation paths and local site effects on the radiated waveforms.

Figure 4 shows the horizontal components of ground acceleration recorded at Sortino and Catania. Several considerations arise from the analysis of this figure. First, the difference between the triggering time of the two instruments (see table II) located at similar focal distance (note that the *S*-waves arrive almost simultaneously at the two sites) which indicates that the accelerograph at Sortino has been not triggered by the first *P*-wave arrival. This implies that the amplitude of the direct *P*-wave is less than 10 gal. A possible explanation for this observation is that Sortino lies on a nodal plane, but this interpretation does not agree with the proposed fault plane solution (Amato *et al.*, 1994; Giardini *et al.*, 1994). Second, the amplitudes of *S*-waves recorded at Catania are $2 \div 3$ times larger than those recorded at Sortino. We might interpret this observation as the effect of local site response, as the Catania instrument is located on alluvial sands and clays. However, the coda amplitudes on the two accelerograms are similar (see fig. 4), sug-

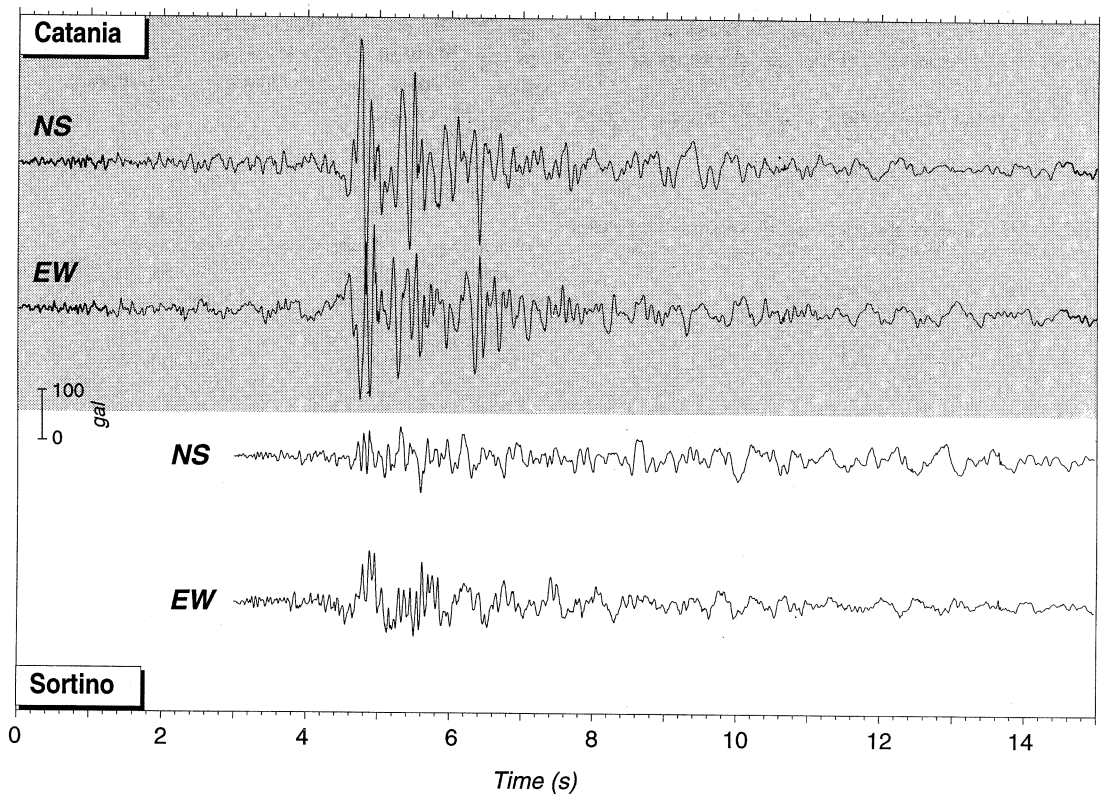

Fig. 4. Horizontal components of ground acceleration recorded at Catania and Sortino. Waveforms have been aligned with respect to their triggering times.

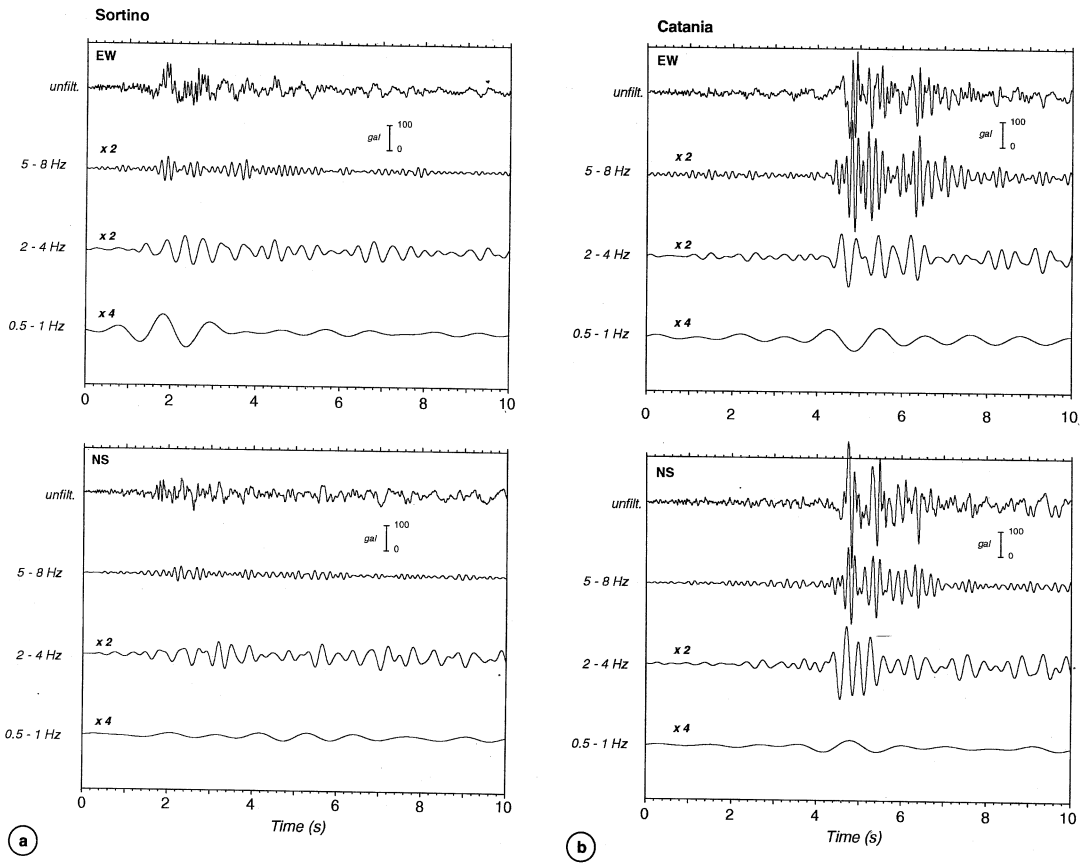

Fig. 5a,b. Band-pass filtered horizontal components of ground acceleration at Sortino (a) and Catania (b). The upper trace in each box is the unfiltered accelerogram. The scale reduction with respect to the amplitude scale is indicated by the numbers written on the waveforms.

gesting that directivity effects or frequency-dependent amplifications of direct *S*-waves due to impedance variations along the propagation path (Boore, 1986) must be invoked to explain the observed time histories. Third, the lack of low frequencies on the NS component recorded at Sortino is evident. Figure 5a,b shows the comparison between the band-pass filtered horizontal components recorded at Sortino and Catania, respectively. This figure points out that the amplification of seismic waves at the Catania site is evident at high frequencies ($f > 2$ Hz) and within the *S*-wave time window. Moreover, the low frequency amplitudes ($f < 1$ Hz) at Sortino are fully polarized on the EW component, confirming the lack of low frequency content on the NS component.

The analysis of *S*-wave polarization confirms that the polarization angle of *S*-waves at Sortino, computed in different frequency bandwidths, ranges between 90° and 100°, while the *S*-wave polarization of the Catania accelerogram ranges between 120° and 140°, confirming that *S*-waves are mostly polarized on the EW component at Sortino. Figure 6 shows the displacement pulses computed using the de-

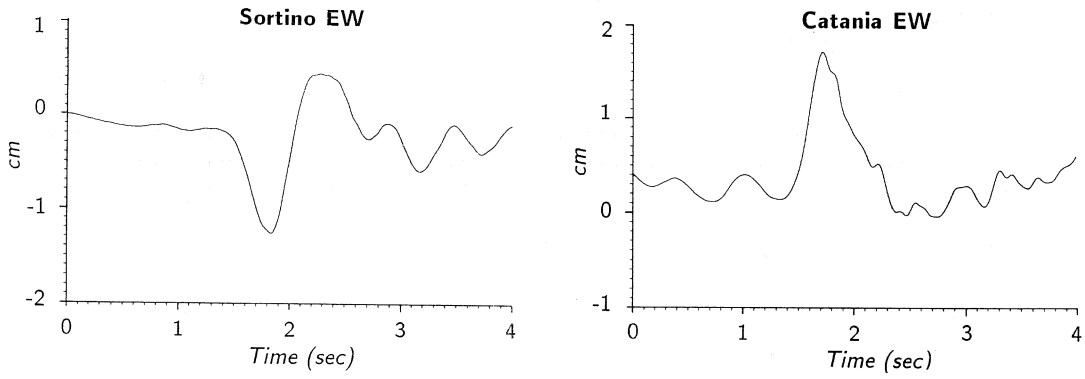

Fig. 6. EW displacement waveforms at Sortino and Catania. The duration of the main pulse is about 0.75 s on both the signals.

convolution technique proposed by Alessandrini *et al.* (1990) from the Sortino and the Catania EW horizontal acceleration time series. Note that the EW component of the accelerogram recorded at Sortino is very close to the direction of maximum polarization. For both pulses the duration is about 0.75 s, indicating that the corner frequency is close to 1 Hz.

A problem that arises from the analysis of *S*-wave polarization is the consistency of the *S*-wave polarization angles with those estimated from the CMT focal mechanism (fig. 1) and the earthquake location proposed by Amato *et al.* (1994). The errors in the take-off angle and azimuth associated to the uncertainties in the hypocenter location cannot explain the disagreement between observed and computed *S*-wave polarization. Errors in the computation of fault plane solutions may be invoked to explain this contradiction. However, our interpretation is that strong crustal heterogeneities present in the area affect the propagation of seismic waves during their paths from the source to the recording sites.

5. Spectral analysis

In this section, we analyze the *S*-wave acceleration spectra in order to evaluate source and attenuation parameters for the 1990 Eastern Sicily earthquake. The *S*-wave spectra of ground acceleration were computed after the deconvolution for the instrumental response (Alessandrini *et al.*, 1990). The observed spectra are fitted with an omega-square model currently used by many authors (Boore, 1986; Houston and Kanamori, 1986; Sommerville *et al.*, 1987; Chael, 1987 among many others), and already applied to the accelerograms written by several recent Italian earthquakes (Rovelli *et al.*, 1988; Cocco and Rovelli, 1989; Rovelli *et al.*, 1991).

The theoretical *S*-wave acceleration spectrum is expressed as

$$A(f, R) = S(f)\frac{e^{-\pi\kappa f}}{R} \qquad (5.1)$$

where $S(f)$ is the ω^2 source spectrum (Aki, 1967; Brune, 1970)

$$S(f) = CM_0\frac{(2\pi f)^2}{1+\left(\frac{f}{f_c}\right)^2},$$

and C

$$C = \frac{F_s R_{\theta,\varphi}}{4\pi\rho\beta^3}$$

is a constant including the free surface factor ($F_s = 2$) and the rms radiation pattern for each horizontal component ($R_{\theta,\varphi} = 0.63/\sqrt{2}$); $\rho = 2.7$ g/cm^3 and $\beta = 3.3$ km/s are the mean values of the density and S-wave velocity in the crust, respectively. M_0 and f_c are the seismic moment and the corner frequency (Aki, 1967; Brune, 1970; Hanks and Kanamori, 1979). The source parameters M_0 and f_c are related to the stress drop $\Delta\sigma$ by the following equation (Brune, 1970; Boore, 1983)

$$f_c = 4.9 \times 10^6 \beta \left(\frac{\Delta\sigma}{M_0} \right)^{\frac{1}{3}} \qquad (5.2)$$

where β is in km/s, $\Delta\sigma$ in bar and M_0 is expressed in dyne·cm. Equation (5.1) includes the geometrical spreading factor $1/R$ (where R is the hypocentral distance) and the anelastic attenuation $e^{-\pi\kappa f}$ (Anderson and Hough, 1984) described by the parameter

$$\kappa = \int_{\gamma} \frac{ds}{v(s)\,Q(s)}$$

where v and Q are the wave velocity and the quality factor along the propagation path γ, respectively. As the smallest values of Q are generally found in the shallower layers of the crust, the κ value is controlled mostly by the near-receiver anelastic properties (Anderson and Hough, 1984; Rovelli *et al.*, 1988).

The evaluation of the spectral parameters begins with the estimate of κ. Following Anderson and Hough (1984), the κ value is computed estimating the decay of the log-spectrum of ground acceleration versus frequency, in the frequency band $f^* < f < f_{max}$; f^* and f_{max} are the frequency of the maximum spectral amplitude and the maximum frequency of the observed data ($f_{max} \approx 20$ Hz) depending on the signal-to-noise ratio. The assumption of an ω^2 source spectrum implies that the acceleration spectrum is flat at frequencies larger than the corner frequency f_c. In this case κ represents only the contribution of anelastic attenuation. Because we are analyzing the acceleration spectra in a limited frequency bandwidth ($\Delta f \approx 20$ Hz), we must stress that, if the source spectrum is not flat at frequencies larger than f_c (an ω^3 source spectrum implies a ω^{-1} a high frequency decay), the estimate of κ is biased by the source contribution. For this reason the evaluation of the attenuation parameter κ is model dependent. However, the spectral model stated by eq. (5.1) provides a satisfactory fit of the acceleration spectra observed in different tectonic regions (Boore, 1986; Houston and Kanamori, 1986; Rovelli *et al.*, 1988; Cocco and Rovelli, 1989; Rovelli *et al.*, 1991); consequently, we interpret the estimates of κ in terms of anelastic attenuation properties. The estimated κ values are listed in table III. These values range between 0.033 s and 0.045 s, with the exception of the higher values obtained for Licata (0.15 s) and Giarre (0.084 s). The estimate of κ from the Licata accelerogram is affected by a site amplification at low frequencies which causes an overestimation of the high frequency spectral decay; the high value of κ estimated at Licata can be also interpreted in terms of the considerable high frequency attenuation properties of the thick Quaternary sediments under the station. The Giarre station is located on the Etna volcanic complex, therefore a strong attenuation of S-waves is expected due to the volcanic roots. The mean value, computed excluding the Licata and the Giarre estimates, is $\kappa = 0.040 \pm 0.005$ s, where the uncertainty is expressed by one standard deviation.

The second step consists in estimating the corner frequency after the correction of each acceleration spectrum for geometrical spreading and for anelastic attenuation as described by the parameter κ. The procedure proposed by Andrews (1986) was applied to the corrected spectra in order to estimate the corner frequency f_c:

$$f_c = \frac{1}{2\pi} \sqrt{\frac{I_V}{I_D}}$$

where

$$I_V = \int_{f_{min}}^{f_{max}} V^2(f)\, df$$

and

$$I_D = \int_{f_{min}}^{f_{max}} D^2(f)\, df$$

$V(f)$ and $D(f)$ are the velocity and the displacement spectra, respectively, considered in the frequency band from $f_{min} \approx 0.5$ Hz up to $f_{max} \approx 20$ Hz. The estimated values of f_c are listed in table III. They range between 0.9 Hz and 1.9 Hz with a mean value of $f_c = 1.3$ Hz, computed assuming a log-normal distribution. The corner frequency value estimated from the acceleration spectra observed at Sortino (see table III) is very close to the average value. Moreover, the value $f_c = 1.3$ Hz gives a source duration $T \simeq \frac{1}{f_c}$ equal to 0.8 s, close to the values obtained from the displacement pulses of Catania and Sortino (fig. 6).

The seismic moment M_0 was estimated from the strong motion data using a one-parameter inversion, which minimizes the following error function

$$\chi^2 = \sum_{k=1}^{N} \left(\log \ddot{U}(f_k) - \log A(f_k, R)\right)^2$$

where $\ddot{U}(f_k)$ is the observed acceleration spectrum at the N discrete frequencies f_k, while

$$A(f_k, R) \propto M_0$$

and the proportionality constant is fixed by the pre-determined values of κ for each station (table III) and f_c (1.3 Hz). The seismic moment estimates are listed in table III. The method used in this study to evaluate separately the corner frequency and the seismic moment was preferred to the simultaneous inversion to avoid the bias between the source parameters (both these methods are model dependent). The estimated seismic moments range between 0.8×10^{24} dyne·cm and 1.8×10^{24} dyne·cm, where the minimum value comes from the Sortino recording (rock site) and the maximum value comes from the Catania recording (site on alluvial sediments). For this earthquake Giardini *et al.* (1994) estimated a seismic moment value of $M_0 = 3.7 \times 10^{24}$ dyne·cm by inverting the long period waveforms recorded at regional distances by the seismic stations of the MEDNET network. This value is 4.5 times larger than that estimated from strong motion data at Sortino. A value of $M_0 = 0.8 \times 10^{24}$ dyne·cm corresponds to a moment magnitude of $M = 5.2$ using the scale defined by Hanks and Kanamori (1979), while $M_0 = 3.7 \times 10^{24}$ dyne·cm leads to a moment magnitude of $M = 5.7$. The moment magnitude values are lower than the local magnitude $M_L = 5.9$ estimated on the strong motion accelerograms. The two estimates of M_0, resulting from strong motion and regional broad-band data, and the f_c value discussed before yield to stress drop values ($\Delta\sigma$ in eq. (5.2)) larger than 500 bars. The high stress drop could explain the difference between the moment magnitude (ranging between $M = 5.2$ and $M = 5.7$) and the local magnitude $M_L = 5.9$.

Figures 7a,b show the fit of horizontal components of acceleration spectra by means of the theoretical curves computed from eq. (5.1) using the average values of the corner frequency ($f_c = 1.3$ Hz), the average κ (0.04 s), and the two values of seismic moment resulting from local ($M_0 = 0.8 \times 10^{24}$ dyne·cm) and regional data ($M_0 = 3.7 \times 10^{24}$ dyne·cm). Moreover, because the estimate of seismic moment from strong motion data depends on the corner frequency, in figs. 7a,b we add the plot of the theoretical spectra computed for the seismic moment value resulting from regional broad-band data and for a corner frequency value of 0.6 Hz, that is roughly half the value previously estimated. This latter theoretical spectrum was computed in order to account for possible errors in the estimates of corner frequency. Di Bona and Rovelli (1988) discuss the effects of the bandwidth limitation on the estimates of corner frequency using the Andrews (1986) method. They show that the limited frequency bandwidth can affect the computation of the integrals of ground motion, producing an overestimation of corner frequency when f_c is close to the lower limit of the available frequency band. This effect can explain the ambiguity on the corner frequency evaluation.

Figures 7a,b show that the theoretical spectra computed using the largest seismic moment

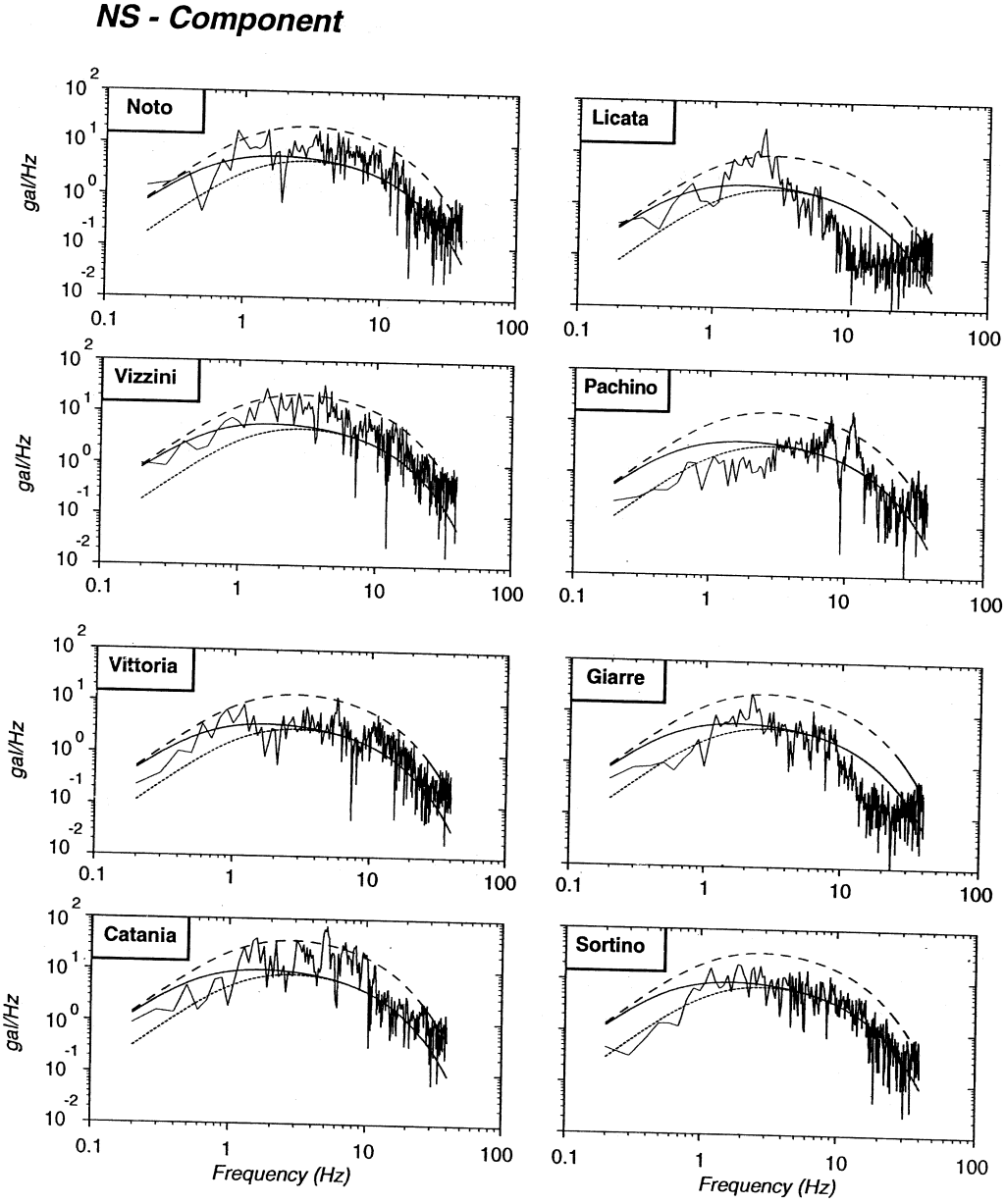

Fig. 7a. Comparison between the horizontal components of observed acceleration spectra and the theoretical curves obtained by the spectral model of eq. (5.1). Dashed curve represents the theoretical spectrum computed for a corner frequency of f_c = 1.3 Hz and a seismic moment of $M_0 = 3.7 \times 10^{24}$ dyne·cm. The dotted curve shows the spectrum for the same value of corner frequency but a seismic moment of $M_0 = 0.8 \times 10^{24}$ dyne·cm. The solid curve represents the theoretical spectrum computed for a corner frequency value of 0.6 Hz and the seismic moment ($M_0 = 3.7 \times 10^{24}$ dyne·cm) resulting from broad-band regional data. A value of κ equal to 0.04 s has been used to compute all the theoretical spectra plotted in this figure.

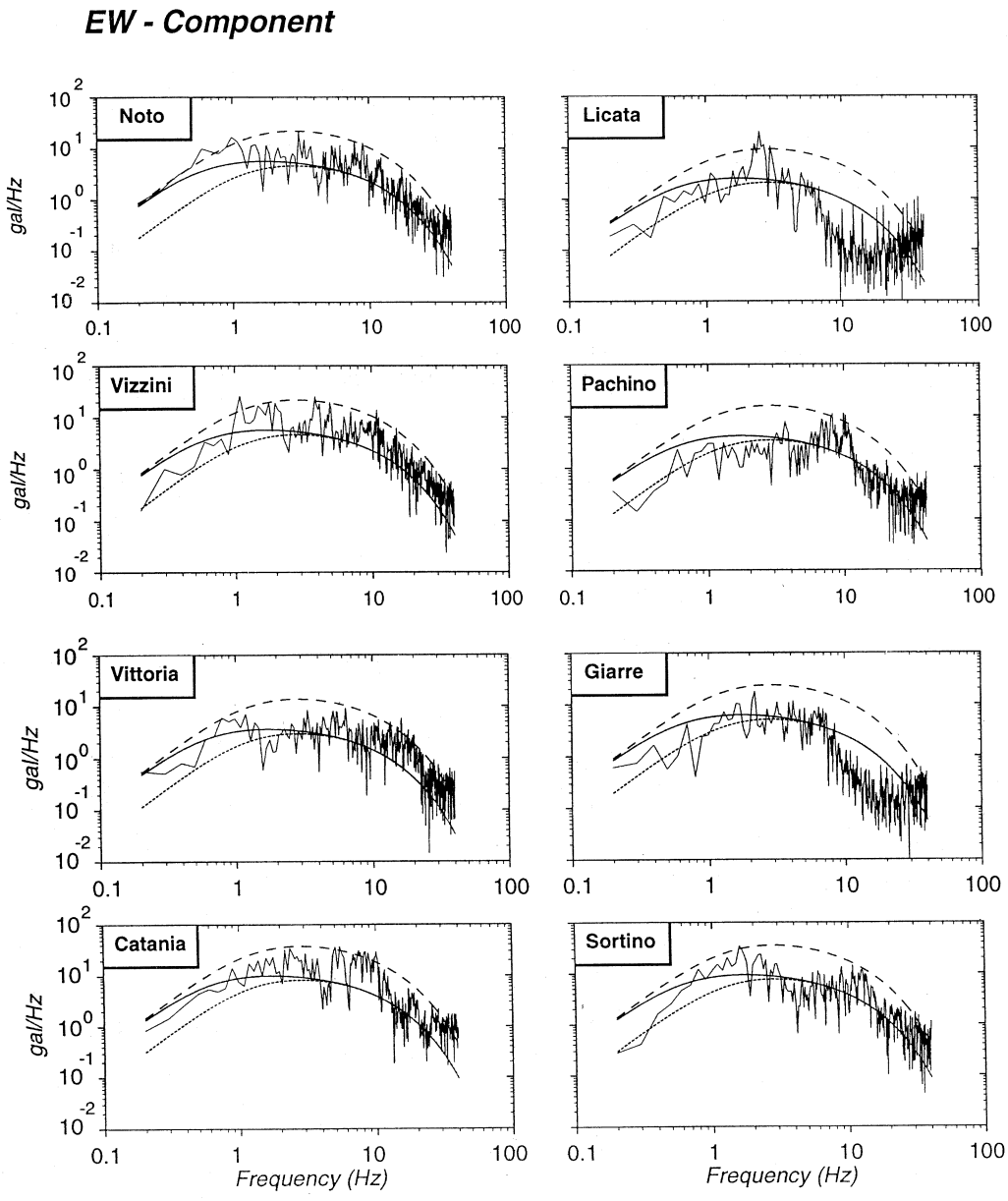

Fig. 7b. Comparison between the horizontal components of observed acceleration spectra and the theoretical curves obtained by the spectral model of eq. (5.1). Dashed curve represents the theoretical spectrum computed for a corner frequency of f_c = 1.3 Hz and a seismic moment of $M_0 = 3.7 \times 10^{24}$ dyne·cm. The dotted curve shows the spectrum for the same value of corner frequency but a seismic moment of $M_0 = 0.8 \times 10^{24}$ dyne·cm. The solid curve represents the theoretical spectrum computed for a corner frequency value of 0.6 Hz and the seismic moment ($M_0 = 3.7 \times 10^{24}$ dyne·cm) resulting from broad-band regional data. A value of κ equal to 0.04 s has been used to compute all the theoretical spectra plotted in this figure.

value (from regional data) and a corner frequency of 1.3 Hz overestimate the observed spectra over the whole available frequency band, even if they reproduce the low frequency spectral amplitudes at some stations (Noto and Vittoria). On the contrary, the theoretical spectra computed by using the seismic moment value resulting from strong motion data ($M_0 = = 0.8 \times 10^{24}$ dyne·cm) and a corner frequency of 1.3 Hz produce a good fit of the observed spectra only at high frequencies. Noteworthy is the observation that the theoretical spectra computed by reducing the corner frequency by a factor of 2 and for the seismic moment from regional broad-band data provide the best fit over the whole frequency band. It is important to note that the two sets of values for seismic moment and corner frequency (f_c = 0.6 Hz, $M_0 = 3.7 \times 10^{24}$ dyne·cm and f_c = 1.3 Hz, $M_0 = 0.8 \times 10^{24}$ dyne·cm) predict the same flat level of the acceleration spectrum (that is proportional to $M_0 f_c^2$), but the lower corner frequency value provides a better fit of the low frequency spectral amplitudes. The stress drop associated to f_c = 0.6 Hz and $M_0 = 3.7 \times 10^{24}$ dyne·cm is $\Delta\sigma$ = 210 bars.

Our conclusion is that the acceleration spectra observed during the 1990 Eastern Sicily earthquake cannot be modelled over the whole frequency band by assuming a simple omega-square spectral model. Both source complexities and local site amplifications affect the spectral content of the observed ground motion.

6. Discussion

The analysis of the strong-motion data produced by the Eastern Sicily earthquake emphasizes the role played by crustal heterogeneities and near-receiver amplifications due to the surface geology and topography. This is inferred from two observations: 1) peak ground accelerations are sensibly different for stations at comparable distances from the source, and 2) local magnitude values (at least 5.9) are significantly higher than the estimated values at regional distance (5.4). Moreover, the spectral analysis (figs. 7a,b) shows that the spectral shape is extremely variable among the different sites, and it is difficult to evaluate the source contribution properly, without evaluating the site response of each recording site due to local geology.

Figure 8a-c shows the peak values of acceleration, velocity and displacement versus the hypocentral distance. The curves drawn on the figure are the empirical relations obtained by Sabetta and Pugliese (1987) from the analysis of the strong-motion data recorded for several Italian earthquakes. The Sabetta and Pugliese (1987) empirical curves are evaluated for a moment magnitude of M = 5.7 corresponding to the seismic momemt $M_0 = 3.7 \times 10^{24}$ dyne·cm. On the average, the peak ground accelerations versus the hypocentral distance (fig. 8a) are larger than the values predicted by Sabetta and Pugliese's relation. In particular, the peak ground accelerations from Catania and Licata are sensibly larger than the predicted values. Both these recording sites are characterized by a soft Holocene-sediment filling.

It is noteworthy that all the observed peak ground velocities overestimate the values predicted by the empirical relation. This is the consequence of the large low-frequency amplitudes that dominate when ground acceleration is integrated. The extension of this frequency band is extremely variable among the observed spectra. Figure 8a-c shows that peak ground displacements are less scattered than peak ground acceleration and velocity.

The empirical relations proposed by Sabetta and Pugliese (1987) to predict peak ground velocity and acceleration underestimate the peak values observed during the 1990 Eastern Sicily earthquake. The magnitude of the 1990 earthquake is within the magnitude range in which the empirical regressions have been computed. However, a moment magnitude of 5.7 is not sufficient to reproduce the observed peak ground motions, enhancing the role played by local site amplifications and propagation paths. This also explains why the local magnitude from strong motion data (M_L 5.9) overestimates the value resulting from regional broad-band data (M_L 5.4).

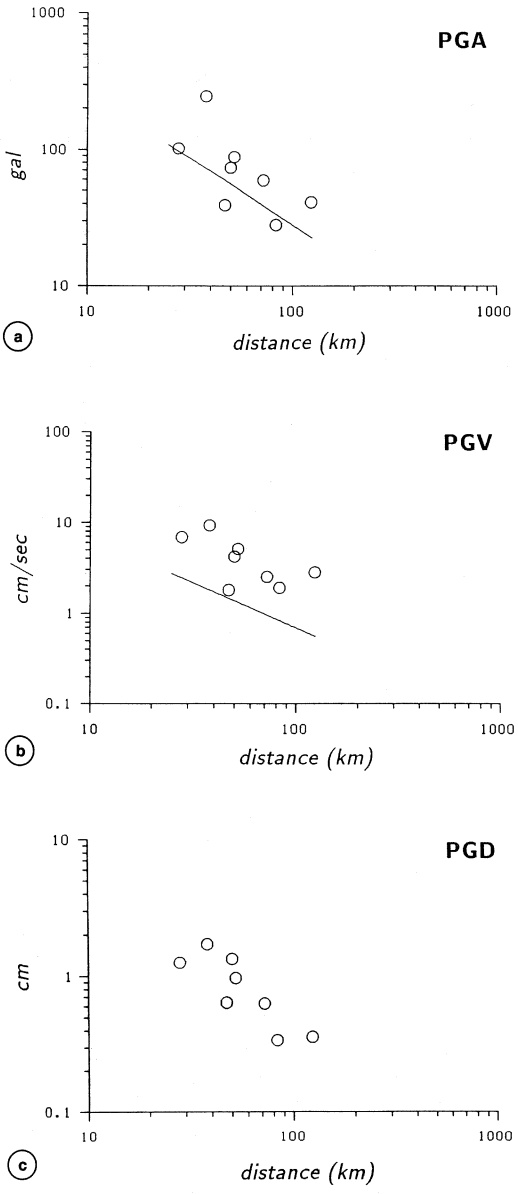

Fig. 8a-c. Peak values of acceleration (a), velocity (b) and displacement (c) versus the hypocentral distance. The solid lines represent the empirical curves proposed by Sabetta and Pugliese (1987). These curves have been computed for a moment magnitude M = 5.7 resulting from the Hanks and Kanamori (1979) relationship with a seismic moment of $M_0 = 3.7 \times 10^{24}$ dyne·cm.

A possible interpretation of the misfit between theoretical and observed spectra (figs. 7a,b) could be a weak correction for seismic attenuation. Rovelli *et al.* (1988) and Cocco and Rovelli (1989) represented the *S*-wave attenuation by using two terms: the $e^{-\pi\kappa f}$, that represents the anelastic absorption due to the intrinsic Q_i, and a second attenuation term which describes the loss for scattering and complexity of propagation due to fluctuations of the elastic properties of the medium $e^{\frac{-\pi f T}{Q_s}}$. By assuming $Q_s = Q_0 f$, the second attenuation term becomes $e^{\frac{-\pi R}{cQ_0}}$ (see Rovelli *et al.*, 1988 for further details). The value of Q_0, estimated for different Italian regions, is Q_0 = 100. This value yields an attenuation of the observed spectrum (the correction is frequency independent) at 30 km of 25%, and it becomes more important at hypocentral distances of 100 km (about 60%). These observations demonstrate that the fit of the observed spectra at the closest (≈ 30 km) stations (Sortino and Catania), with the higher seismic moment value (M_0 = = 3.7×10^{24}), cannot be improved by including the $e^{\frac{-\pi R}{cQ_0}}$ term in the analitical expression of the theoretical spectrum (eq. (5.1)). Because of the absence of Q_0 estimates appropriate for Eastern Sicily, we avoided including the frequency independent attenuation term in eq. (5.1). We conclude that the ambiguity in the appropriate values of source parameters to be used for theoretical modelling of observed spectra cannot be solved by modifying the parameterization of seismic attenuation.

7. Conclusions

We have estimated the source and the attenuation parameters from the strong motion accelerograms recorded during the 1990 Eastern Sicily earthquake. The local magnitude estimated from the strong motion accelerograms, by synthesizing the Wood-Anderson response is M_L = 5.9, at a rock site (Sortino) 30 km away from the epicenter. This value is higher than the magnitude estimated at regional distance from broad-band seismograms that is

M_L = 5.4 (Giardini *et al.*, 1994). The local magnitudes computed at the other strong motion sites are higher than the value resulting for Sortino.

The strong-motion data were used to estimate the attenuation parameter κ, the seismic moment M_0, and the corner frequency f_c. The value of κ is 0.040 ± 0.005 s, and it is lower than the values estimated in other regions in Italy (Rovelli *et al.*, 1988 and 1991; Cocco and Rovelli, 1989). This implies low attenuation properties of the Iblean platform, where most of the strong motion stations are located. The seismic moment estimated from the accelerograms recorded at Sortino (rock site) is $M_0 = 0.8 \times 10^{24}$ dyne·cm, that is the smallest value among those computed at the other sites. The seismic moment estimated at regional distance by inverting the broad-band waveforms is $M_0 = 3.7 \times 10^{24}$ dyne·cm (Giardini *et al.*, 1994). The corner frequency estimated from the spectral analysis is 1.3 Hz, and it seems to be consistent with the duration of the displacement pulses at Sortino and Catania (fig. 6). However, the analysis of observed acceleration spectra points out that a lower corner frequency value (0.6 Hz) improves the fit on the whole available frequency band when the seismic moment from regional data is used. It is important to note that corner frequency values of the order of 0.6 Hz have been estimated for earthquakes of similar size ($3.5 \leq M_0 \leq 4.0 \times 10^{24}$ dyne·cm) in other seismogenic areas in Italy (see Rovelli *et al.*, 1988). Assuming a corner frequency f_c = 1.3 Hz, the stress drop ranges from 500 bars to 2 kbars for the two extreme seismic moment estimates, while a value of 0.6 Hz reduces the stress drop to 210 bars when the largest value of seismic moment is used. The moment magnitude ranges from M = 5.2 (for $M_0 = 0.8 \times 10^{24}$ dyne·cm) to M = 5.7 (for $M_0 = 3.7 \times 10^{24}$ dyne·cm) depending on the seismic moment value used in the Hanks and Kanamori (1979) empirical relation. The moment magnitude is lower than the local magnitude resulting from the strong motion accelerograms (M = 5.9). Because of the uncertainties in the estimate of Brune stress drop (210 bars $\leq \Delta\sigma <$ 2 kbars), we interpret the difference between the moment magnitude ($5.2 \leq M \leq 5.7$) and the strong motion magnitude (5.9) in terms of weak attenuation properties of the Iblean platform, where most of the stations are located.

The peak ground accelerations and velocities observed at the strong-motion sites at different hypocentral distances are higher than the values predicted for an earthquake of magnitude M = 5.7 by the empirical relationship proposed by Sabetta and Pugliese (1987). This result agrees with the high level of damage caused by the shock, and the wide area in which the earthquake was felt. The behavior of peak values of ground motion versus hypocentral distance points out the role played by local site amplifications, and propagation effects on the observed time histories.

The comparison between the observed spectra of ground accelerations and the theoretical curves computed from an omega-square spectral model including anelastic attenuation and geometrical spreading (eq. (5.1)) further confirms that local site amplifications affect the spectral shape of the observed ground acceleration in the frequency band $2 < f < 10$ Hz. This is particular evident at several sites (see fig. 5a,b) such as Licata, Pachino, Vizzini, Noto and Catania.

However, the comparison of acceleration time histories and spectra recorded at Catania and Sortino points out the role played by the crustal heterogeneities (such as lateral heterogeneities) along the propagation paths of seismic waves from the source to the recording sites. In fact, the effect of local site amplifications at high frequencies ($2 < f < 10$ Hz) at the Catania site can easily be modelled by means of a simple 1-D model using the Haskell-Thompson algorithm. However, the local site response cannot explain the inconsistency between observed and theoretical *S*-wave polarization and the amplification of direct *S*-wave, with respect to the coda amplitudes, at Catania.

These observations can be explained as the effect of crustal heterogeneities on the propagation of seismic waves or as the effect of complexities of the seismic source. These effects complicate the analysis of ground acceleration recorded at the Sortino rock site.

Acknowledgements

We would like to thank Roberto Fregonese, Alessandro Amato, Giulio Selvaggi, Domenico Giardini and N. Alessandro Pino for helpful discussions and for their criticism. We thank Aldo Zollo for reviewing this manuscript and for his criticism. We thank Daniela Riposati for drawing many of the figures.

REFERENCES

AKI, K. (1967): Scaling law of seismic spectrum, *J. Geophys. Res.*, **72**, 1217-1231.

ALESSANDRINI, B., A. ROVELLI, M. COCCO and S. MAZZA (1990): Computation of ground displacement from strong-motion accelerograms using the exact deconvolution technique, *Bull. Seismol. Soc. Am.*, **80**, 1753-1761.

AMATO, A., R. AZZARA, A. BASILI, C. CHIARABBA, M. COCCO, M. DI BONA and G. SELVAGGI (1994): Main shock and aftershocks of the December 13, 1990, Eastern Sicily earthquake, *Annali di Geofisica*, **38**, 255-266 (this volume).

ANDERSON, J.G. and S.E. HOUGH (1984): A model for the shape of the Fourier amplitude spectrum of acceleration at high frequencies, *Bull. Seismol. Soc. Am.*, **74**, 1969-1993.

ANDREWS, D.J. (1986): Objective determination of source parameters and similarity of earthquakes of different size, *Earthquake Source Mechanics Ewing Series*, edited by S. DAS *et al.* (AGU, Washington, D.C.), **6**, 259-267.

BONAMASSA, O. and A. ROVELLI (1986): On distance depedence of local magnitudes found from Italian strong-motion accelerograms, *Bull. Seismol. Soc. Am.*, **76**, 579-581.

BOORE, D.M. (1983): Stochastic simulation of high-frequency ground motions based on seismological models of the radiated spectra, *Bull. Seismol. Soc. Am.*, **73**, 1865-1894.

BOORE, D.M. (1986): Short period *P*- and *S*-wave radiation from large earthquakes: implications for spectral scaling relations, *Bull. Seismol. Soc. Am.*, **76**, 43-64.

BRUNE, J.N. (1970): Tectonic stress and the spectra of seismic shear waves from earthquakes, *J. Geophys. Res.*, **75**, 4997-5009 (and correction, *J. Geophys. Res.*, **76**, 5002).

CHAEL, E.P. (1987): Spectral scaling of earthquakes in the Miramichi region of New Brunswik, *Bull. Seismol. Soc. Am.*, **77**, 347-365.

COCCO, M. and A. ROVELLI (1989): Evidence for the variation of stress drop between normal and thrust faulting earthquakes in Italy, *J. Geophys. Res.*, **94**, 9399-9416.

COCCO, M., A. AMATO, R. AZZARA, A. BASILI, E. BOSCHI, C. CHIARABBA, M. DI BONA, D. GIARDINI, N.A. PINO, A. ROVELLI and G. SELVAGGI (1991): The December 13, 1990, Eastern Sicily earthquake (M_L 5.4), *Eos* (Trans. Amer. Geophys. Un.), 311.

DI BONA, M. and A. ROVELLI (1988): Effects of the bandwidth limitation on stress drops estimated from integrals of the ground motion, *Bull. Seismol. Soc. Am.*, **78**, 1818-1825.

GIARDINI D., B. PALOMBO and N.A. PINO (1994): Long-period modelling of MEDNET waveforms for the December 13, 1990 Eastern Sicily earthquake, *Annali di Geofisica*, **38**, 267-282 (this volume).

HANKS, T.C. and H. KANAMORI (1979): A moment magnitude scale, *J. Geophys. Res.*, **84**, 2348-2350.

HOUSTON, H. and H. KANAMORI (1986): Source spectra of great earthquakes: teleseismic constraints on rupture processes and strong motion, *Bull. Seismol. Soc. Am.*, **76**, 19-42.

HUTTON, L.K. and D.M. BOORE (1987): The M_L scale is Southern California, *Bull. Seismol. Soc. Am.*, **77**, 2074-2093.

KANAMORI, H. and P.C. JENNINGS (1978): Determination of local magnitude, M_L, from strong motion accelerograms, *Bull. Seismol. Soc. Am.*, **68**, 471-485.

ROVELLI, A., O. BONAMASSA, M. COCCO, M. DI BONA and S. MAZZA (1988): Scaling laws and spectral parameters of the ground motion in active extensional areas in Italy, *Bull. Seismol. Soc. Am.*, **78**, 530-560.

ROVELLI, A., M. COCCO, R. CONSOLE, B. ALESSANDRINI and S. MAZZA (1991): Ground motion waveforms and source spectral scaling from close-distance accelerograms in a compressional regime area (Friuli, Northeastern Italy), *Bull. Seismol. Soc. Am.*, **81**, 57-80.

SABETTA, F. and A. PUGLIESE (1987): Attenuation of peak horizontal acceleration and velocity from Italian strong-motion records, *Bull. Seismol. Soc. Am.*, **77**, 1491-1513.

SOMMERVILLE, P.G., J.P. MCLAREN, L. V. LEFEVRE, R.W. BURGER and D. V. HELMBERGER (1987): Comparison of source scaling relations of Eastern and Western North American earthquakes, *Bull. Seismol. Soc. Am.*, **77**, 322-346.